Structural, electrical, optical, and mechanical characterizations of decorative ZrO_xN_y thin films

P. Carvalho, F. Vaz,[a] L. Rebouta, L. Cunha, C. J. Tavares, and C. Moura
Departamento de Física, Universidade do Minho, 4800-058 Guimarães, Portugal

E. Alves
Departamento de Física, Instituto Tecnológico Nuclear, Estrada Nacional 10, 2686-953 Sacavém, Portugal

A. Cavaleiro
ICMES—Fac. Ciências Tecnologia Universidade de Coimbra, 3030-039 Coimbra, Portugal

Ph. Goudeau, E. Le Bourhis, and J. P. Rivière
Laboratoire de Métallurgie Physique, Université de Poitiers, 86960 Futuroscope, France

J. F. Pierson
Dpt CREST, Institut FEMTO-ST [UMR Centre National de la Recherche Scientifique (CNRS) 6174], Université de Franche-Comté, 25211 Montbéliard Cedex, France

O. Banakh
University of Applied Sciences, Haute École ARC, 7, Avenue de l"Hotel-de-Ville, 2400 Le Locle, Switzerland

(Received 7 March 2005; accepted 7 June 2005; published online 28 July 2005)

The main objective of this work is the preparation of decorative zirconium oxynitride, ZrO_xN_y, thin films by dc reactive magnetron sputtering. Film properties were analyzed as a function of the reactive gas flow and were correlated with the observed structural changes. Measurements showed a systematic decrease in the deposition rate with the increase of the reactive gas flow and revealed three distinct modes: (i) a metallic mode, (ii) a transition mode (subdivided into three zones), and (iii) an oxide mode. The measurements of target potential were also consistent with these changes, revealing a systematic increase from 314 to 337 V. Structural characterization uncovered different behaviors within each of the different zones, with a strong dependence of film texture on the oxygen content. These structural changes were also confirmed by resistivity measurements, whose values ranged from 250 to 400 $\mu\Omega$ cm for low gas flows and up to 10^6 $\mu\Omega$ cm for the highest flow rates. Color measurements in the films revealed a change from bright yellow at low reactive gas flows to red brownish at intermediate flows and dark blue for the films prepared at the highest flows. Hardness measurements gave higher values for the region where larger grain sizes were found, showing that the grain growth hardening effect is one of the main parameters that can help explain the observed behavior. Also the peak intensity ratio and the residual stress states were found to be important factors for explaining this behavior. © *2005 American Institute of Physics*.
[DOI: 10.1063/1.1990261]

I. INTRODUCTION

In the last few years an emergent field of research involving the so-called decorative thin films is gaining more and more importance. Colored films on high-quality consumer products are supposed to provide both scratch resistance and protection against corrosion, while enhancing their appearance due to surface attractive colorations. Regarding the apparent colorations of thin films, one must distinguish between the inherent colorations (e.g., nitrides, carbonitrides, or borides) and apparent colorations due to interference effects (e.g., transparent oxide or ultrathin absorbing films).[1] Since the apparent colorations of interference films are primarily influenced by their thickness,[2] their use appears to be a less suitable choice as decorative coatings. However, the increasing demand for low-cost products and reduced material resources is moving research towards the development of deposition procedures that will provide the basis for different colored films, with minimum use of resources. In this sense, the continuous change in deposition procedures, such as material targets and/or reactive gas changes, to obtain different colored films is c1early not suitable.

Recently, a c1ass of materials, the metal oxynitrides thin films, MeO_xN_y (Me=early transition metal),[1,3–7] is gaining importance in several technological applications. These are also being investigated for decorative applications. Their relevance arises from the fact that the presence of oxygen allows the tailoring of film properties between those of metallic nitrides, MeN, and those of the correspondent insulating oxides, MeO_x. Tuning the oxide/nitride ratio allows one to tune the band gap, bandwidth, and crystallographic order between oxide and nitride and hence the electronic and optical properties of materials, including color.

The main purpose of this work consists of the preparation of colored films, based on single-layered zirconium ox-

[a]Author to whom correspondence should be addressed; electronic mail: fvaz@fisica.uminho.pt

ynitrides, ZrO_xN_y. Elucidating the relationship between color and the corresponding physical, structural, and mechanical properties is an important goal of this work.

II. EXPERIMENTAL DETAILS

ZrO_xN_y thin films were deposited onto high-speed steel (AISI M2), stainless-steel (AISI 316), and single-crystal silicon (100) substrates by reactive dc magnetron sputtering in a laboratory-size deposition system.[8] It consisted of two vertically opposed rectangular magnetrons (unbalanced of type 2), in a closed field configuration.[9] The films were prepared with the substrate holder positioned at 70 mm in all runs, using a dc density of 100 A m^{-2} on the zirconium target (99.6 at. %). A gas atmosphere composed of argon (working gas) and nitrogen + oxygen (19:1 ratio) reactive mixture was used for the depositions. The Ar flow was kept constant at 55 SCCM (standard cubic centimeter per minute) and the mixed reactive gas flow rate varied from 4 to 17.5 SCCM. The working pressure was approximately constant at 0.4 Pa and the substrates were grounded. The pumping speed was adjusted for 356 l/s. The atomic composition of the as-deposited samp1es was measured by Rutherford backscattering spectroscopy (RBS) using a 2-MeV He^+ beam as well as 1.4- and 2-MeV proton beams to increase the accuracy in the oxygen signals. The analyzed area was about 0.5×0.5 mm^2. In addition, for some samples, particle-induced x-ray emission (PIXE) measurements were performed to check for impurities. Ball crater tests were used to measure the thickness of the samples. In order to examine the film structure, x-ray-diffraction (XRD) experiments were undertaken in a Philips PW 1710 apparatus, using Cu $K\alpha$ radiation. Glancing incidence x-ray-diffraction (GIXRD-θ=2°) experiments were also performed on some selected samples, where the phase indexing revealed some doubts. Electrical resistivity was deduced from sheet resistance measurements at room temperature, using the four-point probe method. The characterization of film's color was computed using a commercial MINOLTA CM-2600d portable spectrophotometer (wavelength range: 400–700 nm), using diffused illumination at an 8° viewing angle. The spectrophotometer was equipped with a 52-mm diameter integrating sphere and three pulsed xenon lamps. Color specification was computed under the standard CIE illuminant D65 (specular component excluded) and represented in the CIELAB 1976 color space.[10,11] Film's hardness and Young's modulus were determined from the loading and unloading curves, carried out with an ultralow load-depth sensing Berkovich nanoindenter from CSM Instruments (Switzerland). Poisson's ratio of 0.3 was used for the calculations. The maximum load used was 30 mN, with a loading time of 30 s, holding 30 s, and unloading in 30 s, producing an average number of 15 indentations per sample. The residual stresses were calculated using Stoney's equation,[12] after measuring the parabolic deflections of the thin substrates (AISI 316) by laser triangulation, before and after deposition of the films.

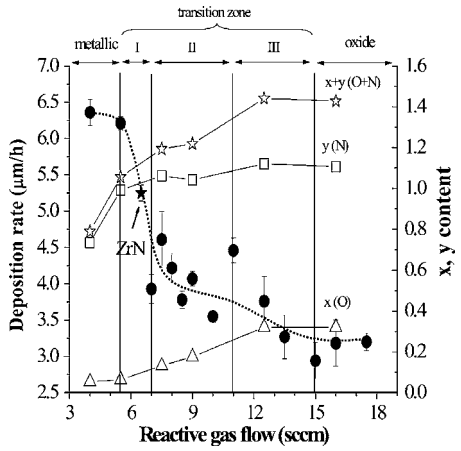

FIG. 1. Variation of the deposition rate of the ZrO_xN_y films as a function of the reactive gas flow. The figure also shows the amount of oxygen, nitrogen, and their sum (normalized to the amount of zirconium). The solid circles correspond to the deposition rate.

III. RESULTS

The film thicknesses ranged from 3 to 4 μm and their oxygen and nitrogen contents (normalized to the zirconium content) will be noted in the text as x and y, respectively. The variation of the deposition rate with the reactive gas flow is plotted in Fig. 1. The figure shows that the evolution of the deposition rate can be divided into three different modes (regimes): (i) a metallic mode, (ii) a transition mode (which is subdivided in three distinct zones), and (iii) an oxide mode. The distinct zones within the transition mode are directly correlated with the structural features of the films. The first regime—metallic mode—includes the group of samples prepared with reactive gas flows from 4 to 5.5 SCCM, with an atomic ratio of nonmetallic to metallic atoms, (N+O)/Zr, lower than and close to 1, exhibiting color appearances from metallic color towards light silver yellow, which is characteristic of sub-stoichiometric zirconium nitride films, ZrN_x. In these low reactive gas flows, the sputtering process is in the metallic regime, resulting in higher deposition rates. For reactive gas flows between 5.5 and 15 SCCM there is a transition mode, which can be divided in three distinct zones, the transition zones I, II, and III, as it will be shown later by different analyses. In these transition zones, the deposition rate decreases continuously and tends to stabilize at the highest flow rates—the oxide mode. It is important to note that the transition zone I (reactive gas flows from 5.5 up to 7 SCCM) includes the ZrN film (prepared with 6.5 SCCM of pure nitrogen reactive gas), which can be associated with the transition regime between the metallic and compound regimes in the hysteresis cycle of pure nitrides.[13] Additionally, the samples change color from light gold to brownish yellow. The existence of the transition zone II (reactive gas flows between 7 and 11 SCCM) and III (from 11 up to 15 SCCM) is a consequence of the increasing oxygen content of the films. This influence of the oxygen content in the films will be analyzed in more detail later, as well its influence in the other scanned properties. The progressive decrease of the deposition rate within these transition zones is a consequence of the well-known poisoning effect of the target by both

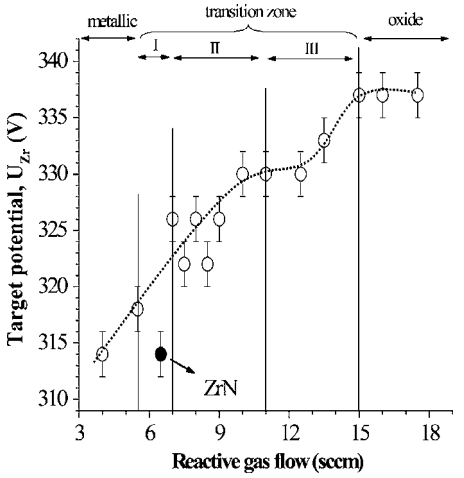

FIG. 2. Variation of the zirconium target potential as a function of the reactive gas flow.

reactive gases.[2] Both zirconium nitride and oxide layers form at the surface of the Zr target. Since the sputtering yield of both compounds is lower than that of Zr, a decrease in the deposition rate is expected. From this increasing poisoning, the deposition rate falls from ~6.5 to ~3 μm/h. The evolution of the deposition rate with the reactive gas flow is also well correlated with the change of the concentration of nonmetallic elements, $x+y$, as can be seen in Fig. 1. The metalloid content is lower than 1 for the depositions performed in the metallic mode, increasing to about 1 in the transition zone I, to about 1.2 in the transition zone II, and finally rises to about 1.4, when going from transition zone III to the films deposited at highest reactive gas flows (oxide mode). The above-mentioned target poisoning effect, based on measurements of the Zr target potential, is shown in Fig. 2. For very low reactive gas flows, all the available gas is consumed and the target potential is roughly constant (U_{Zr} varies from 314 to 318 V), corresponding to the metallic mode regime. With an increase in the reactive gas flow, the target potential progressively rises up to a value close to 337 V, then remains constant for the highest flows, which corresponds to the regime of target poisoning. It is worth of mentioning that the value of target potential for "pure" ZrN was 314 V, which does not follow the growth tendency, due to the absence of oxygen in the reactive gas during its preparation. The presence of oxygen in the oxynitride samples is certainly a factor that has to be taken into account, since this element affects the sample behavior.

In order to understand the mechanisms of chemical reactions occurring within the different sputtering modes, a detailed structural characterization was carried out. Figure 3 shows the x-ray-diffraction patterns for the samples prepared within the different sputtering modes, where the differences in preferential orientation within each of the zones are clearly visible. For the metallic mode regime, the films crystallize in a B1–NaCl crystal structure, typical for ZrN. Similar behavior was observed in transition zone I, although the peak intensity ratio, I(200)/[I(111)+I(200)] in Fig. 4, is increasing. Hence, indicating some preferential crystalline growth change. This preferred orientation change occurs for

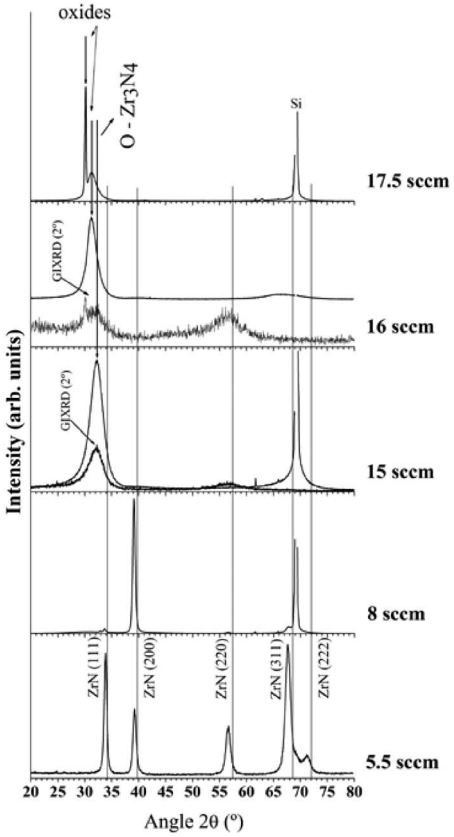

FIG. 3. XRD and GIXRD patterns for five different ZrO_xN_y films. The vertical lines indicate the diffraction peak position of the reference ZrN phase.

the films prepared in intermediate zone II, where the (200) becomes the dominant growth. The effect of the increasing reactive gas and the amount of oxygen (and the correspondent variation in the deposition rate, Fig. 1) is a parameter that influences this variation.

In the literature there are several references to similar texture changes. Wu *et al.*[14] showed that ZrN films (stoichiometric and substoichiometric) grow preferentially ⟨111⟩ oriented, even on different types of substrates. The change of growth direction towards ⟨100⟩ at a high nitrogen partial pressure was also reported by Ramana *et al.*,[15] Gall *et al.*,[16]

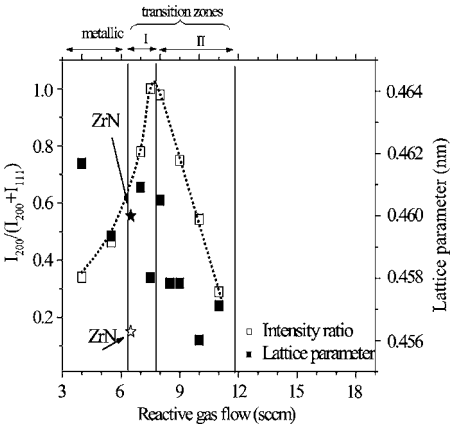

FIG. 4. Variation of the peak intensity ratio and lattice parameter in the films from metallic and intermediate zones I and II, as a function of the reactive gas flow.

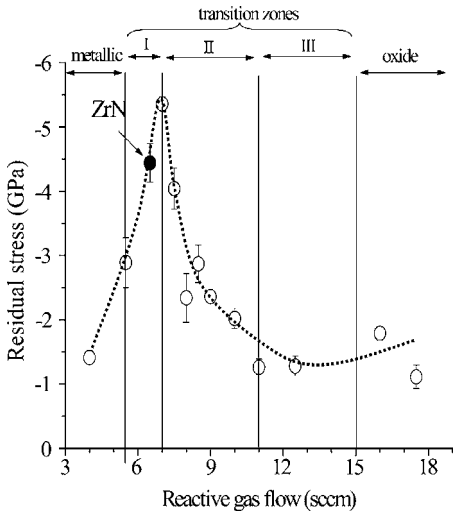

FIG. 5. Film residual stress evolution as a function of the reactive gas flow.

and Shin *et al.*[17] Several models for preferred orientation changes in the sputtered metallic nitride films, MeN (Me =Ti, Zr, Cr, etc.), have been extensively discussed in the literature.[18–21] Pelleg *et al.*[22] and Oh and Je[23] proposed that the preferred orientation in these metallic nitrides is determined by a competition between the two thermodynamic parameters, the tendency to decrease the surface energy and the tendency to decrease the strain energy. Since the (200) planes are associated with the lowest surface energy, a ⟨100⟩ orientation should then be observed at low residual stress conditions.[4] However, these parameters cannot explain themselves all the behaviors, since for some cases of low reactive gas flows, there are also small values of stress for the films exhibiting a ⟨111⟩ orientation.[4] Mahieu *et al.*[24] stated that this change from ⟨111⟩ to ⟨100⟩ can also be the result of distinct growth modes, such as the microstructure changes from zone *T* to zone I, according to Thornton's zone model.[25] These changes were also reported in our previous works as a result of the increasing gas flow.[4]

The ⟨100⟩ orientation within the intermediate zone II is decreasing continuously as can be seen from the peak intensity ratio (Fig. 4). In fact, for a reactive gas flow of 11 SCCM, this parameter is already below 0.4, which shows that the films are mostly randomly oriented. Also the lattice parameter is decreasing significantly within this region. This reduction of lattice parameter is in good agreement with the evolution of the residual stresses (Fig. 5), which follows the same behavior. Indeed, the evolution of the film structure is dependent on the lattice defect formation, such as the oxygen interstitials/substitutions, and the type of crystalline phases (nitride/oxide/oxynitride) that are formed. Moreover, the high residual stresses cannot be attributed to ion bombardment, since the samples were grounded during its preparation. The reason might be in the insertion of oxygen atoms in the ZrN lattice in interstitial (tetrahedrical) positions. However, the insertion of oxygen atoms only happens for low (or intermediate) oxygen content, where in the presence of thermodynamic and kinetic constraints the probability of having oxygen atoms as nearest neighbors to the Zr atoms in the ZrN arrangements is relatively high. Increasing the oxygen content, the concentration of oxygen atoms increases, increasing also the probability of having other oxygen atoms as nearest neighbors, and thus favoring the formation of oxide phases, or other phases, rather than those oxygen-doped nitride phases. This will also decrease the ZrN fcc lattice parameters as well as the residual stress states.

Regarding the x-ray diffractograms for the films prepared with reactive gas flows between 11 and 15 SCCM—transition zone III—the results suggest that the development of a crystalline structure that does not match with that of fcc ZrN. The peak located at $2\theta \approx 32.2°$ presents a shift from the (111) reference ZrN of about 2°. The results from glancing geometry experiments further attested this behavior, while a very broad peak around 56° also appeared. One possibility is that this could be the result of the formation of an oxygen-doped zirconium nitride phase (also with possible nitrogen interstitials), resulting in a structure close to that of Zr_3N_4.[26] The diffraction peak at $2\theta \approx 32.2°$ would then correspond to the (320) plane of that doped Zr_3N_4-type structure or even to a mixture of several peaks predicted in this region for this structure. The peak at $2\theta \approx 56°$ could relate or be a mixture of diffraction peaks predicted for the Zr_3N_4-type structure[16] in the region $2\theta = 54° - 56°$. Several authors have already indicated the shift of the (111) peak of the ZrN (NaCl-type phase) towards smaller angles for the films prepared with high nitrogen flows,[16,27–30] which resulted in the development of a poorly crystallized Zr_3N_4 phase. In the case presented here, the reduced number of diffraction peaks does not allow any further conclusions about the exact nature of the crystalline phase to be made. Furthermore, the flow rate used for the preparation of pure ZrN was about 6.5 SCCM, and in the case of the films from transition zone III, the reactive gas flows used were between 11 and 15 SCCM (more than twice that of pure ZrN). It was also seen, in Fig. 1, that the amount of N+O elements in this third zone is about 1.4, with an amount of nitrogen close to 1.1 (less than that normally present for the development of the Zr_3N_4 phase,[16,27–30] but similar to pure nitrogen reactive atmospheres). This means that if that phase is developed, it probably involves oxygen. In fact, when preparing the ZrN_x films with amounts of reactive gas (pure nitrogen), such as those of the reactive gas mixture used within this transition zone III (between 11 and 15 SCCM), the only phase observed was the one related to ZrN, which means that the oxygen content is ruling this phase transition. According to some authors, this Zr_3N_4 phase (orthorhombic) is formed as a result of cell expansion by incorporation of nitrogen (and oxygen) atoms in interstitial positions.[26,31–33] Other authors have described it as a relaxed NaCl structure with some Zr vacancies.[27,28]

For the films deposited in the oxide mode (with reactive gas flows higher than 15 SCCM), there is another structural change, but again, the reduced number of visible diffraction peaks does not allow a detailed and conclusive analysis. Nevertheless, the diffraction peak at $2\theta \approx 30.1°$ could correspond to the (011) planes of a tetragonal zirconium oxide, ZrO_2, or the (111) planes of a cubic zirconium oxide structure.[34] The diffraction peak at $2\theta \approx 31.3°$ could be assigned to the (111) planes of a zirconium oxide monoclinic-

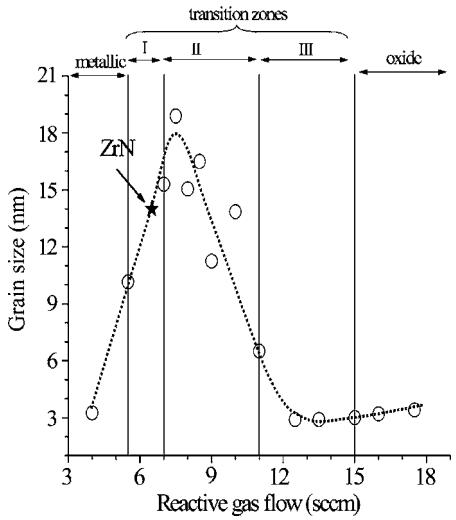

FIG. 6. Change in the film grain size as a function of the reactive gas flow.

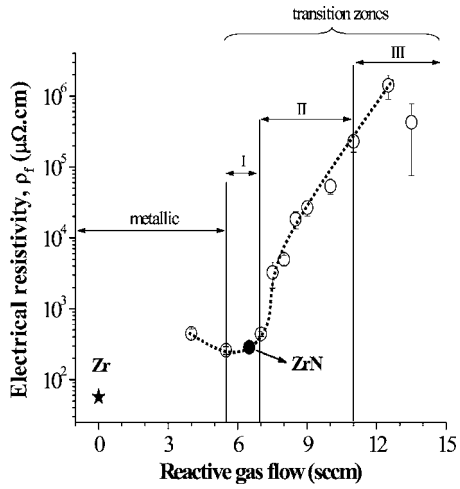

FIG. 7. Variation of film electrical resistivity as a function of the reactive gas flow.

type structure. The possibility of the development of a zirconium oxide orthorhombic structure should also be considered, which would then result from the evolution of that oxygen-doped Zr_3N_4 phase towards an oxide-type one (with possible nitrogen inclusions). The diffraction peak at $2\theta \approx 30.1°$ would then correspond to the (111) planes. Again, the preparation of pure zirconium oxide, ZrO_x, films with increasing oxygen content led to the development of similar mixture of oxide phases, but with higher oxygen flows. This indicates that nitrogen is also influencing the phase evolution, even in this oxide mode. Although the formation of amorphous oxides structures is very often found, several authors claim the formation of both monoclinic and tetragonal oxide phases in the oxide sputtering regime.[35–37] These distinct behaviors in the transition zone III and the oxide mode regime is also seen from Fig. 2, where the target potential grows steadily up to 15 SCCM, the region of the oxygen-doped Zr_3N_4 region, stabilizing for higher flows, the oxide regime.

In order to follow these structural transitions, XRD peak simulation and grain size evaluation, by integral breadth, were carried out (Fig. 6). The results show that the films within transition zone II have larger grains, while the films within transition zone III and in the oxide mode show the smallest ones, revealing an increasing tendency for the films to become amorphous with growing oxygen content (increasing of reactive gas flow). The amount of oxygen is also an important factor for the changes occurring in transition zones I and II. In fact, when preparing the nitride films (only nitrogen in the reactive gas), the transition from $\langle 111 \rangle$ to $\langle 200 \rangle$ growth with increasing gas flow was followed by a decrease in grain size. Similar behavior is also reported in the literature.[16] In the case of the oxynitrides reported here, this transition is followed by an increase in grain size (Fig. 6), showing that it is not just a case of a surface energy minimization dominant process, but also a deformation energy dominant process that is mainly due to the oxygen incorporation in the ZrN lattice and thus the creation of inherent structural defects.

The distinct behaviors occurring within the different zones can also be correlated with the resistivity values (taken at room temperature), as a function of the reactive gas flow (Fig. 7). The initial low values of resistivity are related with the "roughly" metallic nature of the films, with compositions between that of Zr and substoichiometric ZrN(O) (see Fig. 1). The low oxygen content and the similar structure obtained—(111)—for all the films make them very similar in structural terms. The increase of resistivity for reactive gas flows higher than 7 SCCM can be explained by the decrease of the metallic bond contribution and the formation of oxygen-doped ZrN crystalline phase towards a nitrogen-oxygen-rich phase, similar to that of Zr_3N_4. The decrease of the metallic bond contribution can be described by a model of bonding of metal (oxy)nitrides. The electron charges of the transition-metal transfer to nitrogen (and oxygen) forms the transition-metal (oxy)nitride. Accordingly, higher N/Zr and O/Zr atomic ratios result in a higher consumption of the free *d* electrons from zirconium atoms and thus fewer free *d* electrons are available for conduction. This reduction of the number of free electrons decreases the metallic bond contribution and increases the covalent Zr–N and ionic Zr–O bonds,[38] thus increasing the resistivity. Another factor that could decrease the metallic bond contribution[39] and subsequently increasing the resistivity is the growing incorporation of oxygen and nitrogen within the ZrN matrix, which leads to lattice distortions. Finally, another factor that is also important for the increase of resistivity observed for reactive gas flows higher than 7.0 SCCM is the increase of the grain boundaries (grain size is reduced as a function of reactive gas flow in this region and thus the number of grain boundaries increases), which favors the scattering of electrons and thus the increase of resistivity.

The development of an oxygen-doped crystalline phase similar to that of Zr_3N_4, as a consequence of growing incorporation of interstitial atoms (mostly nitrogen, but also possibly oxygen), is consistent with the high values of resistivity within the region, where this insulating phase[25] was identified by XRD. On increasing the gas flow/oxygen contents further on, the films revealed a tendency to develop different structures, which were identified as oxide phases. The occur-

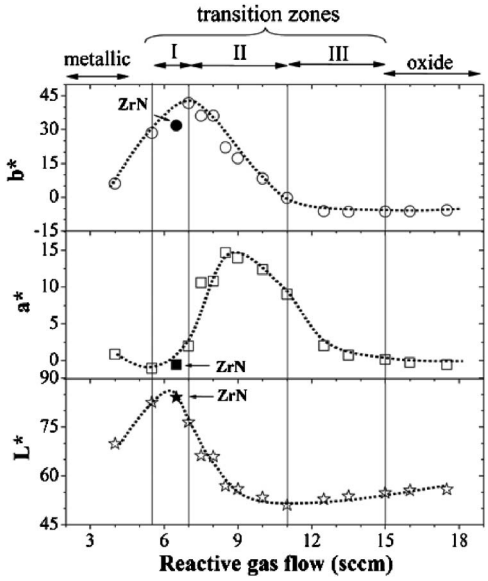

FIG. 8. Average color coordinates in the CIELAB 1976 color space (see Refs. 10 and 11) under the standard CIE illuminant D_{65}, for the films prepared with different reactive gas flows.

rence of these highly insulating phases is also consistent with the fact that it was not possible to measure the resistivity values of these films.

Figure 8 shows the color coordinates L^*, a^*, and b^*, represented in the CIELAB (1976) color space.[10,11] As can be seen from the figure, with increasing flow rate from 4 to 5.5 SCCM (increasing oxygen content), the value of a^* (redness) decreases, while b^* (yellowness) and L^* (brilliance) values increase. The color changes from a very bright yellow pale at the metallic mode to a golden one in transition zone I. With further increase of the flow rate, the film color changes to red brownish (high values of a^*) in transition zone II and dark blue (negative b^* values and relatively low a^* values) at higher flow rates ($\geqslant$11 SCCM). A significant decrease of L^* for the films deposited at flows between 5.5 and 10 SCCM was observed. For reactive gas flows higher than 10 SCCM the L^* coordinate becomes almost constant at a value of about 55. These results indicate a strong influence of the reactive gas flow on film color, which is directly related to the oxygen content in the films.

The optical properties of a material, including its color, are defined by its electronic structure, namely, intra- and interband electronic transitions, occurring during the interaction of material with incident light. The optical properties of the metalliclike Zr–O–N films of transition zone I are dominated by the intraband transitions, due to free electrons. The dielectric function spectra of these films, as measured by spectroscopic ellipsometry, showed a Drude-like behavior, typical for metallic materials, with ε_r negative up to 2.95 eV. The optical parameters (refractive index n and extinction coefficient k taken at 633 nm) of the film deposited at 5.5 SCCM are, respectively, 1.04 and 2.74. With increasing gas flow the contribution of the interband transitions, due to bound electrons, became more pronounced, while the contribution of the intraband transitions is less important. This effect can be observed by the decrease in the brightness (L^*)

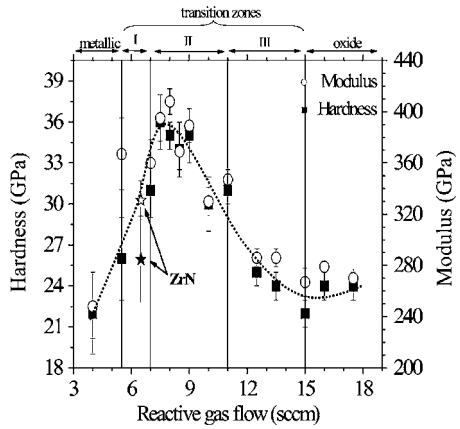

FIG. 9. Hardness and Young's modulus of the sputtered ZrO_xN_y films as a function of the reactive gas flow.

and a progressive shift of ε_r to positive values with increasing gas flow. The optical parameters of the films also evolve with gas flow, n_{633} increases and k_{633} decreases, indicating a decrease in film opacity. The optical parameters n_{633} and k_{633} for the film deposited at 7.5 SCCM are 1.66 and 1.63, and for the film deposited at 9 SCCM, 2.0 and 1.1, respectively.

In the metallic regime, the films exhibit a color, which is between metallic gray (typical for Zr) and golden (characteristic of near-stoichiometric ZrN). In transition zone I (golden films), there is almost no change in the colorimetric coordinates, which is consistent with the presence of the near-stoichiometric ZrN films, and also with the resistivity measurements (Fig. 7). In transition zone II, a reduction of L^*, an increase of a^*, and a reduction of b^* can be explained by the decreasing metallic character of the films (less metallic Zr–Zr bonds). The electron charge transfer from Zr atoms to metalloid (O and N) atoms increases with increasing metalloid content in Zr–O–N. Higher metalloid content results in higher consumption of free d electrons from Zr atoms and less free d electrons are available for conductivity. Consequently, brilliance (L^*) drops with increasing metalloid content. The XRD data of the films in transition zone III and oxide regime (Fig. 3) indicate the development of overstoichiometric nitride (oxide) and oxide phases. The film resistivity values (Fig. 8) become extremely high. The optical properties of these films are governed explicitly by the interband transitions, which are characteristic of semiconducting materials.

The influence of the reactive gas mixture flow variation and its effect on the structural properties of the film can also be correlated with the evolution of its mechanical properties. Figure 9 shows the change in film hardness and Young's modulus as a function of the reactive gas flow. The first noticeable result is the increase in hardness when going from the metallic regime films towards those of transition zones I and II, following the change from a (111) texture to a (200) one. The maximum value of hardness occurs in the second transition zone, which is then followed by a decrease reaching an approximately constant value of about 24 GPa for flows higher than 12 SCCM. It is also worth noting that the region of the highest peak intensity ratio, I(200)/[I(111) +I(200)] (Fig. 4), corresponds to the region of the highest hardness.

Although the structural changes seem to dictate this evolution, Figs. 5 and 6 suggest that other parameters are playing an important role. In fact, there are several works in the literature that try to explain how hardness evolves, taking into account structural parameters, such as the lattice parameter variations, the peak intensity ratio, grain size, residual stresses, and among others.[40] When using ternary nitrides, based on the introduction of an element in a well-known binary nitride, such as here adding oxygen to ZrN, the concentration of the added element is seen as a major parameter with a significant role for the observed behavior. This seems to be also the case here. For low oxygen contents (6–8 at. %), hardness values are very similar to that of pure ZrN. For intermediate oxygen contents there is a maximum in hardness, which can result from oxygen doping of the ZrN lattice, giving rise to a solid solution hardening mechanism. With oxygen insertion, an increased strength of the material due to lattice distortions is expected.[41] The distortion inhibits the mobility of the dislocations, thus inducing an enhancement in hardness. The fact that no bias voltage was used (no ion bombardment) results in low surface mobility and thus the opportunity for oxygen insertions and grain growth (Fig. 6). This figure shows that the grain growth is playing an important role and that the region where larger grain sizes are developed is the one where higher hardness values are obtained.

By comparing the hardness evolution with the trend associated with the residual stress in Fig. 5, one might conclude that beyond these mentioned parameters, the compressive residual stress state of the samples is also a factor to take into account. However, it is clear that stresses are not the only important parameter for the interpretation of the hardness data, since the hardest samples (prepared with gas flows within the region of 7.5–9 SCCM, and having the hardness values ranging from 34 to 36 GPa) show a residual stress decrease from −4.1 to −2.4 GPa. Furthermore, a comparison between Figs. 5 and 9 shows that the hardness can vary from about 25 to ~35 GPa, for the films with residual stresses around −3 GPa. These relatively high residual stresses could be associated with the incorporation of oxygen within the ZrN lattice, which would induce lattice defects in the film structure that act as obstacles for the dislocation motion,[42,43] thus enhancing hardness.

IV. CONCLUSIONS

Thin Zr–O–N films were prepared by dc reactive magnetron sputtering. A systematic decrease in the deposition rate with the increase of the oxygen fraction was observed, revealing the existence of three different sputtering modes—a metallic mode, a transition mode (subdivided in three distinct zones), and an oxide mode. These different modes can be explained by the target poisoning by both reactive gases. The measurements of the target potential are consistent with the changes in the deposition rate. The structural characterization revealed a strong dependence of the film texture on the oxygen content, exhibiting a change from a (111) fcc ZrN-type growth to (200) for low gas flows. On increasing the gas flow (increase of oxygen content), the films tend to develop a structure that might be similar to that of Zr_3N_4 with oxygen inclusions. For relatively high gas flows, the films exhibited only crystalline structures that were indexed as oxide phase. These structural changes were also correlated with the electrical and optical properties of the films (resistivity and color). The initial low values of resistivity are related with the roughly metallic nature of the films, with compositions between that of Zr and substoichiometric ZrN(O). The resistivity of the films increases for reactive gas flows higher than 7 SCCM, which can be explained by the decrease of the metallic bond contribution and the formation of oxygen-doped ZrN crystalline phase towards a nitrogen+oxygen-rich phase, similar to that of Zr_3N_4. The color changes from a very bright yellow pale in the metallic regime to golden one in transition zone I. With further increase of the flow rate, the film color changes to red brownish (high values of a^*) in transition zone II and dark blue (negative b^* values and relatively low a^* values) at higher flow rates ($\geqslant$11 SCCM).

Hardness measurements revealed higher values for the films in the region where larger grains were developed and also a dependence of hardness on the residual stress states. Together with these factors, the structural parameter (XRD peak intensity ratio) and the compositional parameter (oxygen content) are the factors resulting in such behavior.

ACKNOWLEDGMENTS

The work described in this paper is supported by the European Union through the NMP3-CT-2003 505948 project "HARDECOAT." The authors are also grateful to the financial support of the Portuguese FCT institution by the Project No. POCTI/CTM/38086/2001 cofinanced by European community fund FEDER.

[1] R. Franchy, Surf. Sci. Rep. **38**, 195 (2000).
[2] M. Ohring, *The Materials Science of Thin Films* (Academic, New York, 1992).
[3] E. Ariza *et al.*, Thin Solid Films **469–470**, 274 (2004).
[4] F. Vaz *et al.*, Thin Solid Films **469–470**, 11 (2004).
[5] F. Vaz *et al.*, Thin Solid Films **447–448**, 449 (2004).
[6] E. Alves, A. Ramos, N. Barradas, F. Vaz, P. Cerqueira, L. Rebouta, and U. Kreissig, Surf. Coat. Technol. **180–181**, 372 (2004).
[7] F. Vaz, P. Cerqueira, L. Rebouta, S. M. C. Nascimento, E. Alves, Ph. Goudeau, and J. P. Rivière, Surf. Coat. Technol. **174–175**, 197 (2003).
[8] E. Ribeiro, A. Malczyk, S. Carvalho, L. Rebouta, J. V. Fernandes, E. Alves, and A. S. Miranda, Surf. Coat. Technol. **151–152**, 515 (2002).
[9] B. Window and N. Savvides, J. Vac. Sci. Technol. A **4**, 196 (1986).
[10] *Colorimetry*, CIE Publication No. 15 (Commission Internationale de L'Éclairage, Paris, 1971).
[11] *Recommendations on Uniform Color Spaces, Difference-Difference Equations, Psychometric Color Terms*, CIE Publication, Suppl. No. 2–70 (Commission Internationale de L'Éclairage, Paris, 1978).
[12] G. G. Stoney, Proc. R. Soc. London, Ser. A **82**, 172 (1909).
[13] D. A. Glocker and S. Ismat Shah, *Thin Film Process Technology* (Institute of Physics, Bristol, UK, 1995).
[14] D. Wu, Z. Zhang, W. Fu, X. Fan, and H. Guo, Appl. Phys. A: Mater. Sci. Process. **64**, 593 (1997).
[15] J. V. Ramana, S. Kumar, C. David, A. K. Ray, and V. S. Raju, Mater. Lett. **43**, 73 (2000).
[16] D. Gall, S. Kodambaka, M. A. Wall, I. Petrov, and J. E. Greene, J. Appl. Phys. **93**, 9086 (2003).
[17] C. S. Shin, D. Gall, Y. W. Kim, N. Hellgren, I. Petrov, and J. E. Greene, J. Appl. Phys. **92**, 5084 (2002).
[18] R. Lamni, E. Martinez, S. G. Springer, R. Sanjinès, P. E. Schmid, and F. Lévy, Thin Solid Films **447–448**, 316 (2004).

[19]B. Okolo, P. Lamparter, U. Welzel, T. Wagner, and E. J. Mittemeijer, Thin Solid Films **474**, 50 (2005).
[20]Z. B. Zhao, Z. U. Rek, S. M. Yalisove, and J. C. Bilello, Surf. Coat. Technol. **185**, 329 (2004).
[21]J.-H. Huang, K.-W. Lau, and G.-P. Yu, Surf. Coat. Technol. **191**, 17 (2005).
[22]J. Pelleg, L. Z. Zervin, S. Lungo, and N. Croitoru, Thin Solid Films **197**, 117 (1991).
[23]U. C. Oh and J. H. Je, J. Appl. Phys. **74**, 1692 (1993).
[24]S. Mahieu, G. Winter, D. Depla, R. De Gryse, and J. Denul, Surf. Coat. Technol. **187**, 122 (2004).
[25]J. A. Thornton, Annu. Rev. Mater. Sci. **7**, 239 (1977).
[26]D. I. Bazhanov, A. A. Knizhnik, A. A. Safonov, A. A. Bagatur'yants, M. W. Stoker, and A. A. Korkin, J. Appl. Phys. **97**, 044108 (2005).
[27]L. Pichon, T. Girardeau, A. Straboni, F. Lignou, P. Guérin, and J. Perrière, Appl. Surf. Sci. **150**, 115 (1999).
[28]L. Pichon, T. Girardeau, A. Straboni, F. Lignou, J. Perrière, and J. M. Frigerio, Nucl. Instrum. Methods Phys. Res. B **147**, 378 (1999).
[29]H. M. Benia, M. Guemmaz, G. Scmerber, A. Mosser, and J. C. Parlebas, Appl. Surf. Sci. **200**, 231 (2002).
[30]H. M. Benia, M. Guemmaz, G. Scmerber, A. Mosser, and J. C. Parlebas, Appl. Surf. Sci. **211**, 146 (2003).
[31]J. P. Dauchot, S. Edart, M. Wautelet, and M. Hecq, Vacuum **46**, 927 (1995).
[32]M. Yoshitake, T. Nosaka, A. Okamoto, and S. Ogawa, Jpn. J. Appl. Phys., Part 2 **32**, L113 (1993).
[33]B. O. Johansson, H. T. G. Hentzell, J. M. E. Harper, and J. J. Cuomo, J. Mater. Res. **1**, 442 (1986).
[34]J. P. Holgado, J. P. Espinos, F. Yubero, A. Justo, M. Ocana, J. Benitez, and A. R. Gonzalez-Elipe, Thin Solid Films **389**, 34 (2001).
[35]S. Venkataraj, O. Kappertz, H. Weis, R. Drese, R. Jayavel, and M. Wuttig, J. Appl. Phys. **92**, 3599 (2002).
[36]K. Koski, J. Holsa, and P. Juliet, Surf. Coat. Technol. **120–121**, 303 (1999).
[37]S. A. Catledge, M. Cook, Y. K. Vohra, E. M. Santos, M. D. Mcclenny, and K. D. Moore, J. Mater. Sci.: Mater. Med. **14**, 863 (2003).
[38]D. Pilloud, A. S. Dehlinger, J. F. Pierson, A. Roman, and L. Pichon, Surf. Coat. Technol. **174–175**, 338 (2003).
[39]P. Schwarzcopf and R. Kieffer, *Refractory Hard Metals* (Macmillan, New York, 1953), p. 37.
[40]A. Cavaleiro, B. Trindade, and M. T. Vieira, *Nanostructured Coatings—The Influence of the Addition of a Third Element on the Structure and Mechanical Properties of Transition Metal-Based Nanostructured Hard Films; Part I—Nitrides*, edited by J. M. Th. De Hosson and A. Cavaleiro (Kluwer, New York, in press).
[41]D. Sherman and D. Brandon, *Handbook of Ceramic Hard Materials* (Wiley-VCH, New Jersey, 2000).
[42]K. Karlsson, L. Hultman, and J.-E. Sundgren, Thin Solid Films **371**, 167 (2000).
[43]H. Oettel, T. Bertram, V. Weihnacht, R. Wiedemann, and S. V. Zitzewitz, Surf. Coat. Technol. **97**, 785 (1997).